5. Light Extinction In The Desert Southwest

This chapter describes the spatial and temporal variations of light extinction and its components over the study area.

5.1 Principles of Light Extinction

Perception of haze can be influenced by variables such as angle and intensity of the sun, coloration of landscape features, and the distance to the object being viewed. All of these factors are independent of the chemical composition of the air through which objects are viewed. To control for these interfering perception factors, haze is objectively quantified in terms of the light extinction coefficient (b_{ext}). The extinction coefficient is a measure of the total fraction of light that is attenuated per unit distance and has units of inverse megameters (Mm^{-1}). For example, if the light extinction coefficient of the atmosphere is 30 Mm^{-1}, then ~0.003 % of light (λ = 550 nm) will not be transmitted through 1 m of air. Light extinction can be measured directly using a tranmissometer.

The extinction coefficient has contributions from both particles and gases. In equation form, this is expressed as:

$$b_{ext} = b_{sg} + b_{ag} + b_{sp} + b_{ap} \qquad (5\text{-}1)$$

where the subscripts s, a, g, and p refer to scattering, absorption, gases, and particles, respectively. Each component is described briefly below and typical values in the Grand Canyon region are presented. Light scattering and absorption values represent the attenuation of light with a wavelength of 550 nm.

- $\boldsymbol{b_{sg}}$ (light scattering by gases) is also referred to as Raleigh or natural blue-sky scatter. This term is approximately ***11 Mm^{-1}*** at Meadview and is a function of air density (depends upon temperature and pressure, which are strongly dependent upon altitude).

- $\boldsymbol{b_{ag}}$ (light absorption by gases) is primarily due to NO_2 in the atmosphere. This can account for a few percent of the total extinction in urban areas, but is generally insignificant in remote regions such as the Grand Canyon where NO_2 levels are substantially lower. This term is assumed to be ***0 Mm^{-1}*** in this analysis.

- $\boldsymbol{b_{sp}}$ (light scattering by particles) is usually the largest component of the extinction coefficient and is typically dominated by fine particles composed of water, sulfate, nitrate, ammonium, and organic material. Soil and elemental carbon can also scatter light. This is the component in which MPP's sulfur emissions can have the greatest impact. At Meadview from 10/1/91 to 9/30/92, the median DRI nephelometer measurement of b_{sp} was ***8.9 Mm^{-1}***. During the period 7/1/92 to 9/3/92, the median Optec nephelometer b_{sp} at Meadview was ***11 Mm^{-1}***.

- $\boldsymbol{b_{ap}}$ (light absorption by particles) is due to both light absorbing carbonaceous aerosol and soil. b_{ap} was approximated by measuring the absorption of light through a $PM_{2.5}$ sample filter. This measurement is referred to as b_{abs} while the true light absorption by particles is refered to as b_{ap}. The median b_{abs} measurement at Meadview was ***7.2 Mm^{-1}*** during the winter

intensive study and ***6.8 Mm^{-1}*** during the summer intensive study. Note: these values may overestimate the true b_{ap} by up to factor of 2 (see Sections 4.1.3 and 4.2.1.4). Because of this uncertainty, most analyses performed in Project MOHAVE used an estimate of b_{ap} calculated from the elemental carbon concentration instead of using the measured b_{ap} (see Section 6.2).

In this section, results will be presented from transmissometers (b_{ext}), nephelometers (b_{sp}), and particle light absorption through filters (b_{abs}).

5.2 Light Extinction in the Southwest

In terms of light extinction, the Grand Canyon is one of the cleanest Class 1 areas in the United States. Figure 5-1 shows the average annual calculated extinction coefficient throughout the IMPROVE network between March 1992 and February 1995 (Sisler *et al.*, 1996). A region of low background extinction exists throughout Nevada, Utah, Colorado, Wyoming, and Arizona. On a national scale, light extinction was generally higher toward the population centers along the west coast, the Ohio River Valley, and the Chesapeake Bay Area. The lowest annual extinction coefficient was observed at Denali National Park in Alaska.

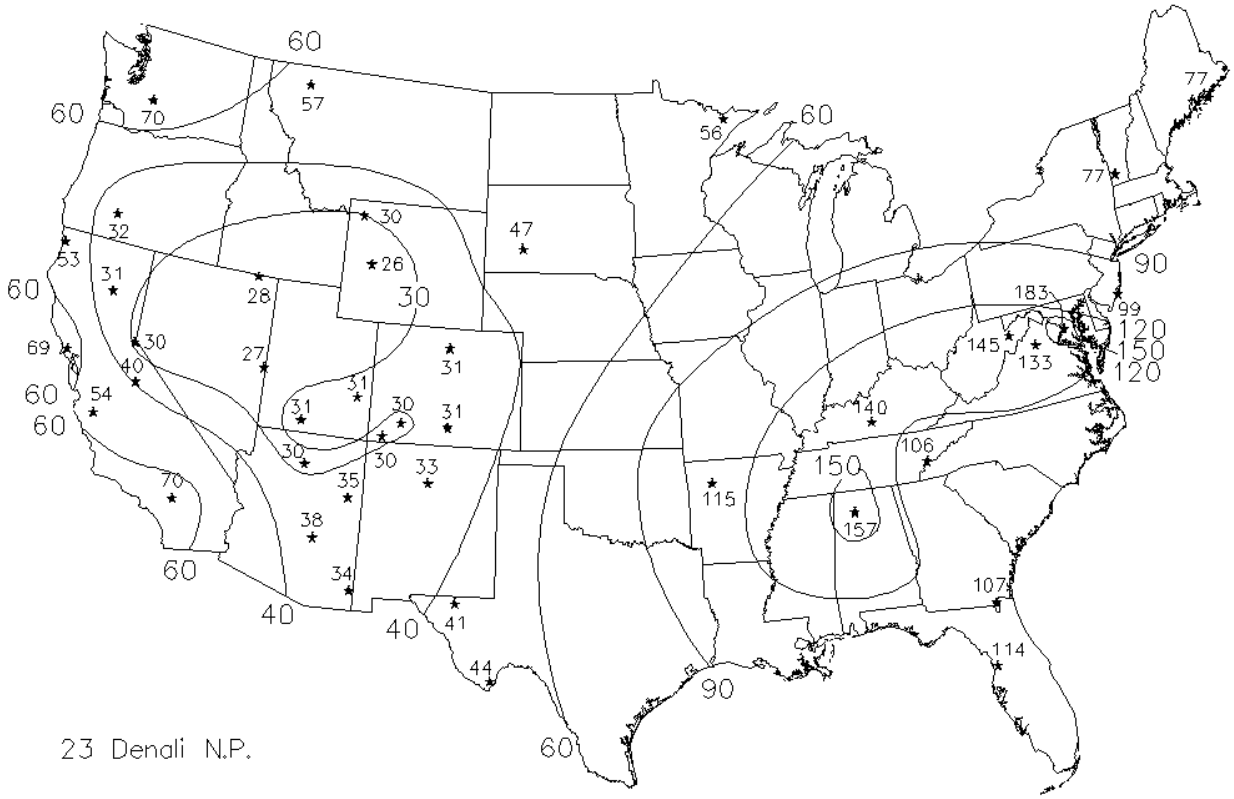

Figure 5-1 Map showing mean annual levels of calculated b_{ext} (in Mm^{-1}) at Class I areas throughout the United States. Data was obtained from the IMPROVE network from particulate matter measurements made between March 1992 and February 1995.

5.3 Haze Levels at the Grand Canyon

Figure 5-2 and Figure 5-3 show the 12-hour average of the transmissometer measured extinction at Meadview (MEAD) and both in (GRCW) and on the rim of (GRCA) the Grand Canyon for the winter and summer intensive study periods. The in-canyon sight path (GRCW) is from Phantom Ranch at the bottom of the Canyon to the South Rim (Grandview Point), with an elevation change of about 1400 m. The South Rim sight path is nearly level (Moran Point to Grandview Point). At least 10 hours of valid data (not influenced by meteorological events such as relative humidity higher than 90%, fog, rain, and blowing dust) were used to calculate each 12-hour averages. The median and maximum b_{ext}, and date of which the maximum b_{ext} occurred are shown in Table 5-1. The values in Table 5-1 were calculated over the intensive sampling periods noted in the table. The episode of high extinction observed in the canyon on 1/10/92 did not occur during this period and was not included at the maximum in the table.

Table 5-1 Summary of 12-hour average Transmissometer Measurements near Grand Canyon National Park.

Site	Winter (1/14/92 – 2/15/92) b_{ext}			Summer (7/12/92 – 9/3/92) b_{ext}		
	Median (Mm^{-1})	Maximum (Mm^{-1})	Maximum Date	Median (Mm^{-1})	Maximum (Mm^{-1})	Maximum Date
MEAD	27.6	42.3	2/2/92 1900	32.5	51.4	8/6/92 1900
GRCA	20.2	31.0	2/4/92 0700	22.7	41.6	8/7/92 0700
GRCW	33.5	39.8	2/2/92 0700	35.5	47.9	7/21/92 0700

Measured extinction was higher within the canyon than at the rim during both winter and summer seasons. The differences between median values at GRCW and GRCA were approximately 13 Mm^{-1} for both seasons. Maximum extinction values at Meadview were higher than either GRCW or GRCA sites. Median and maximum extinction values were higher in summer than in winter at all three sites. Differences in median extinction between winter and summer ranged from 2.0 to 4.9 Mm^{-1}.

It is noteworthy that the maximum extinction periods observed at Meadview and in GCNP are related. During the winter when flows are typically down canyon, the highest measured extinction within the canyon at GRCW was during the day of 2/2/92. The highest 12-hour wintertime extinction at Meadview was measured 12-hours later. Similarly, during the summer intensive study when winds are typically from the south west, the highest 12-hour extinction at Meadview was measured on 8/6/92 in the evening. During the next sampling period, the b_{ext} reached its maximum above the canyon at GRCA. Elevated extinction was also observed within the Grand Canyon at GRCW on 8/7/92. These observations imply that episodes of high extinction are often regional in extent.

There are several reasons why extinction was generally higher within the canyon than at the rim. Sources of pollutants in this region (i.e. population centers and power plants) are generally located at low elevations near water sources. When winds are light, emissions from these areas tend to following natural drainage flows and impact lower elevation monitoring sites. Ventilation of pollutants out of the canyon generally occurs when the lower atmosphere becomes unstable from mid morning to mid afternoon. During the remainder of the day pollutants

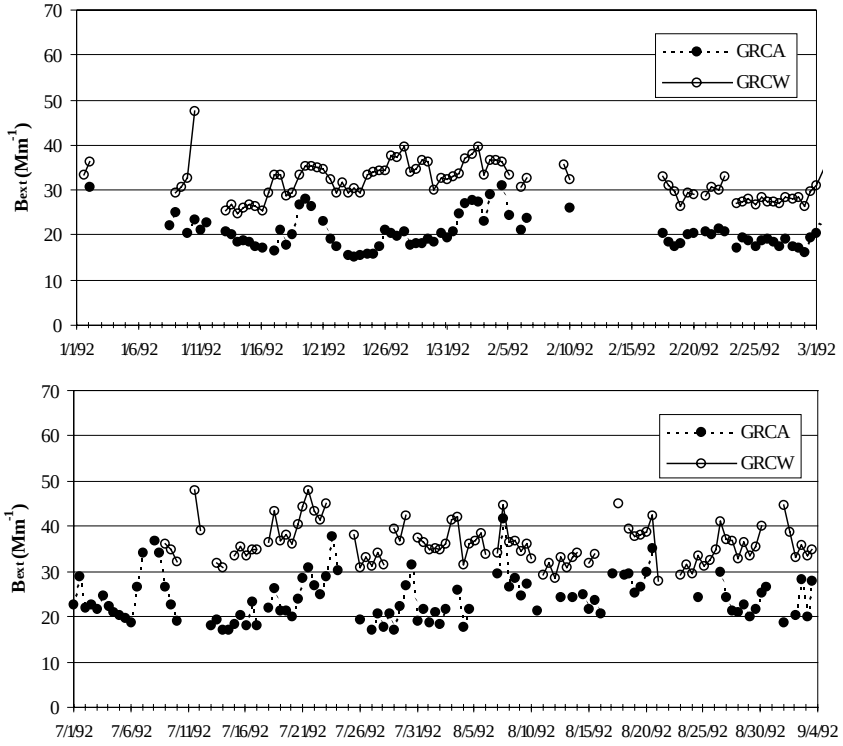

Figure 5-2 Comparison of 12-hour averaged b_{ext} measured in (GRCW) and on the rim of (GRCA) the Grand Canyon.

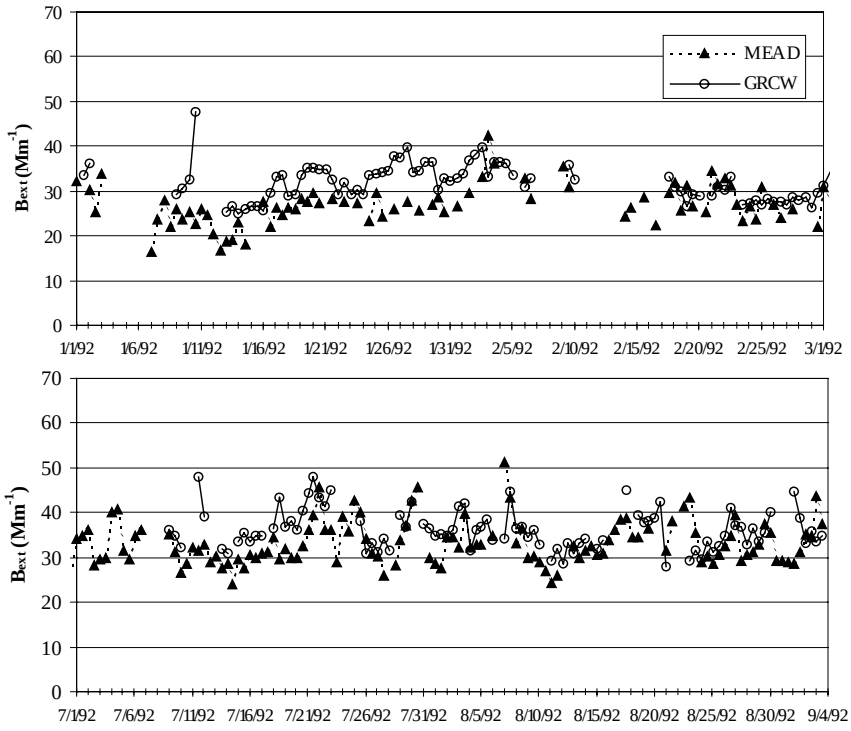

Figure 5-3 Comparison of 12-hour averaged b_{ext} measured at Meadview (MEAD) and within the Grand Canyon (GRCW).

generated at low elevations are frequently confined within the canyon. Consequently, for a large portion of the day, air within the canyon is prevented from mixing with the air above the canyon.

5.4 Diurnal Variation of Light Extinction and Its Components

5.4.1 Light Extinction

The transmissometers measured light extinction at hourly intervals during routine operation. The valid hourly data with weather impacted periods removed are shown in Figure 5-4 and Figure 5-5. With the exception of the transmissometer at Meadview, wintertime light extinction at the Grand Canyon did not exhibit large changes over 12-hour and 24-hour sample durations. (The diurnal variability of the data from Meadview is discussed below.) The summertime extinction signal was more variable at all three sites. There are multiple episodes at each station during the summer in which extinction changes by more than 10 Mm^{-1} over a 3 hour period.

These results suggest that short term impacts to light extinction are frequent during the summer. As a result light extinction attributions to pollution sources averaged over 12 and 24-hour periods may not be representative of the magnitude of the short term impacts.

Figure 5-6 shows hourly averaged light extinction at Meadview measured by transmissometer. Averages were calculated during the intensive studies from valid data measurements collected over periods not influenced by meteorological events such as fog, rain, and blowing dust. The error bars represent the standard error of the hourly measurements.

During the wintertime at Meadview a ~5 Mm^{-1} decrease in measured light extinction was observed during daylight hours between 0900 and 1700. The representativeness of this trend in terms of regional light extinction is questionable since the sight path of the transmissometer was directed through a valley near Meadview. It has been hypothesized that the winter diurnal pattern is due to strong nighttime thermal gradients within the sight path that effectively refract the light from the transmissometer source. This hypothesis is supported by data from a collocated nephelometer at Meadview. Figure 5-7 shows the wintertime diurnal trend of light scattering b_{sp} over the same period as measured by the DRI nephelometer. While a slight reduction (~2 Mm^{-1}) in scattering is observed between 1100 and 1800, the decrease does not seem to be large enough to account for all of the decrease in total light extinction.

Smooth diurnal cycles in light extinction were observed at both GRCW and GRCA. On average, light extinction at the Grand Canyon peaks between 0900 and 1200 during both winter and summer. Diurnal variations typically have a magnitude of ~4 Mm^{-1} at these 2 sites.

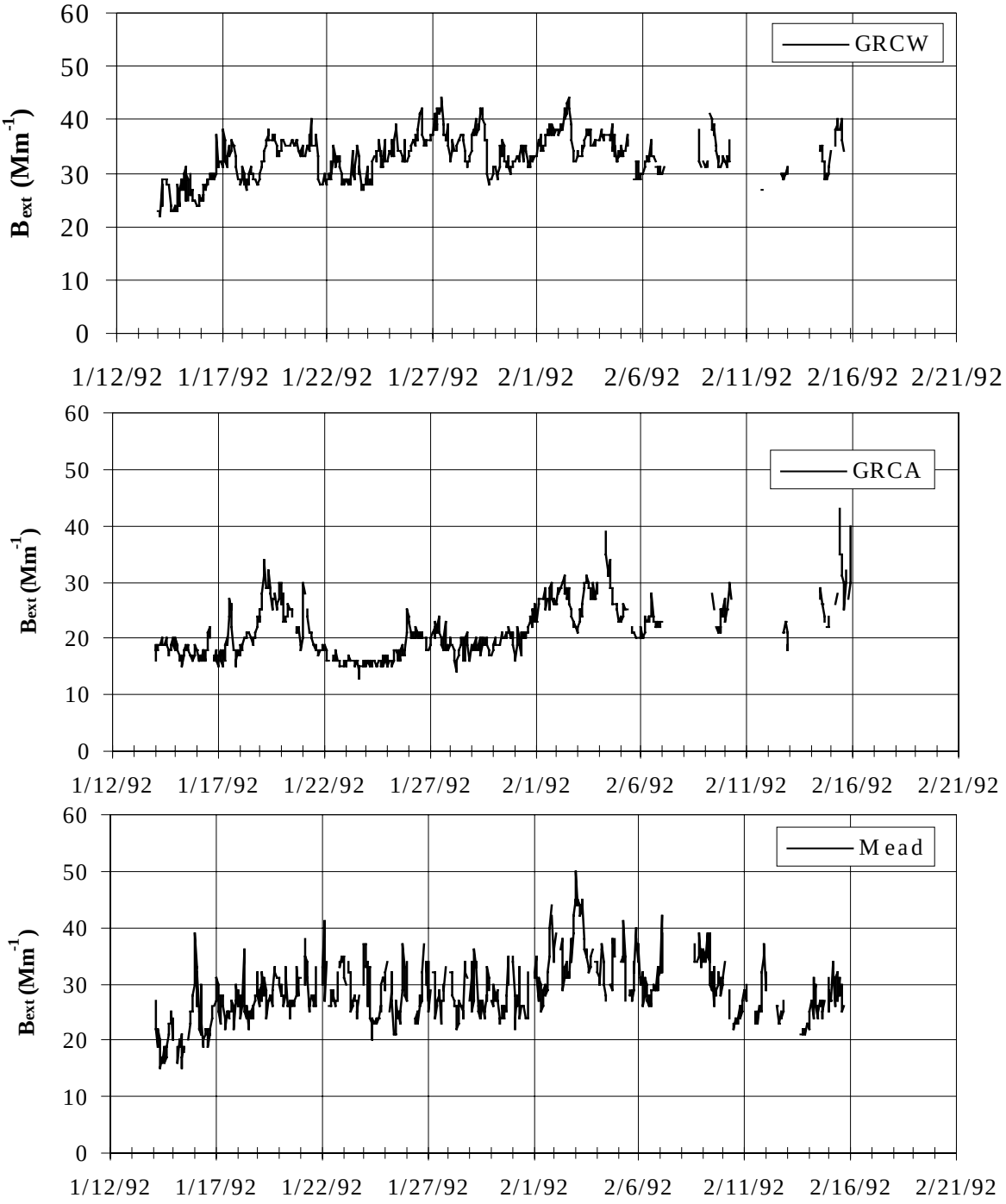

Figure 5-4 Time series of wintertime hourly light extinction at MEAD, GRCA, and GRCW.

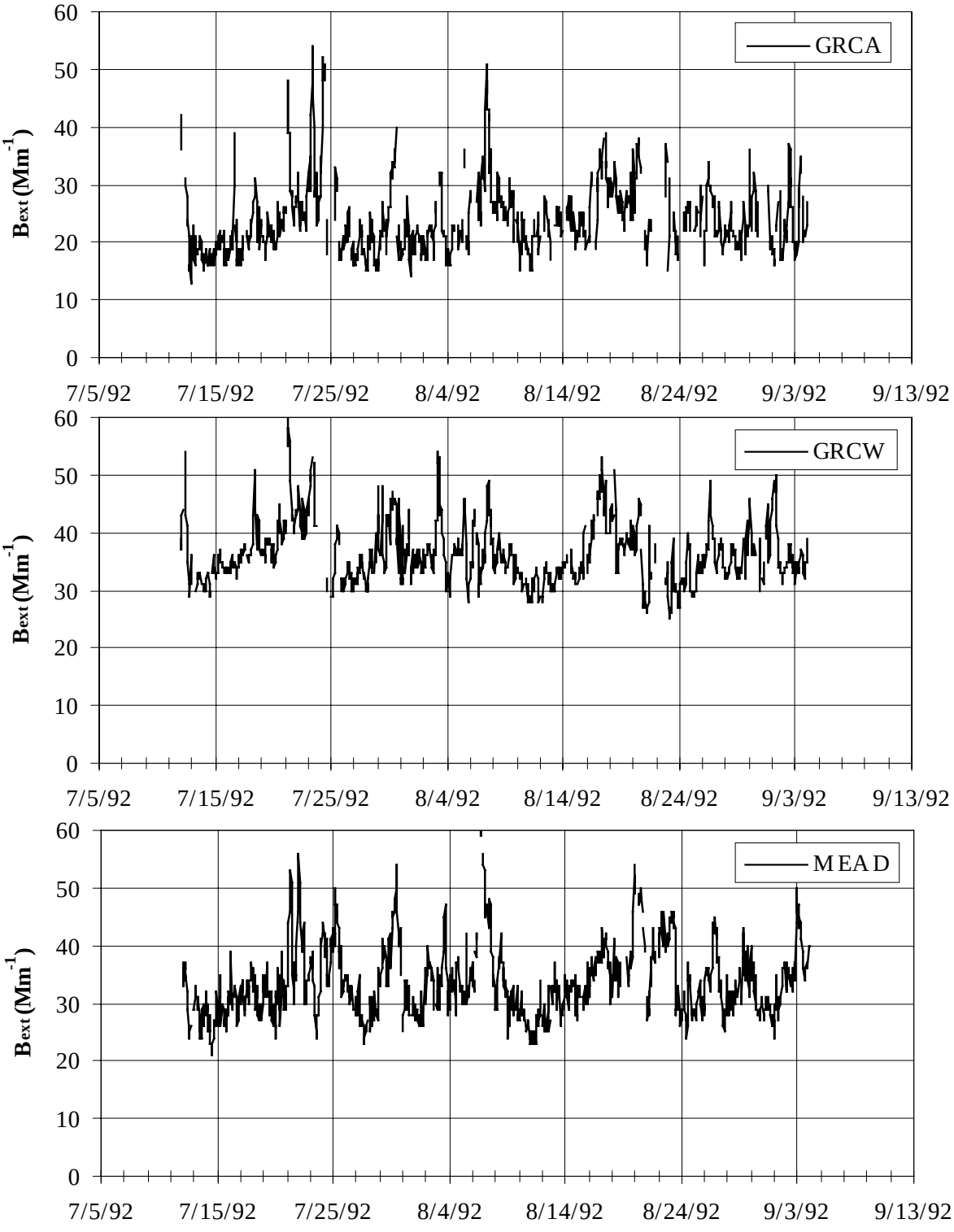

Figure 5-5 Time series of summertime hourly light extinction at MEAD, GRCA, and GRCW.

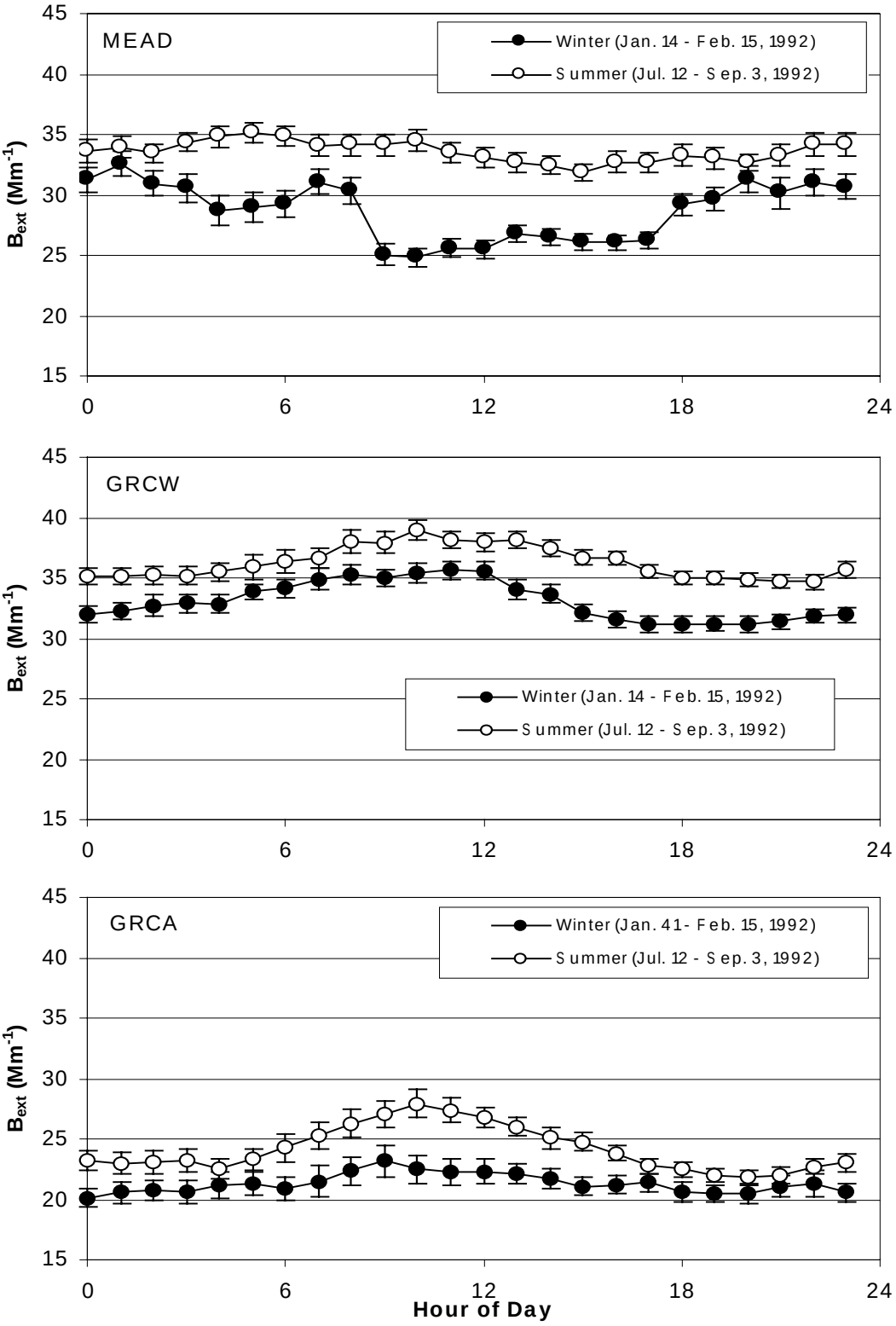

Figure 5-6 Diurnal variation of light extinction on the west side of the Grand Canyon at Meadview (Meadview), within the Grand Canyon (GRCW), and on the south rim of the Grand Canyon (GRCA).

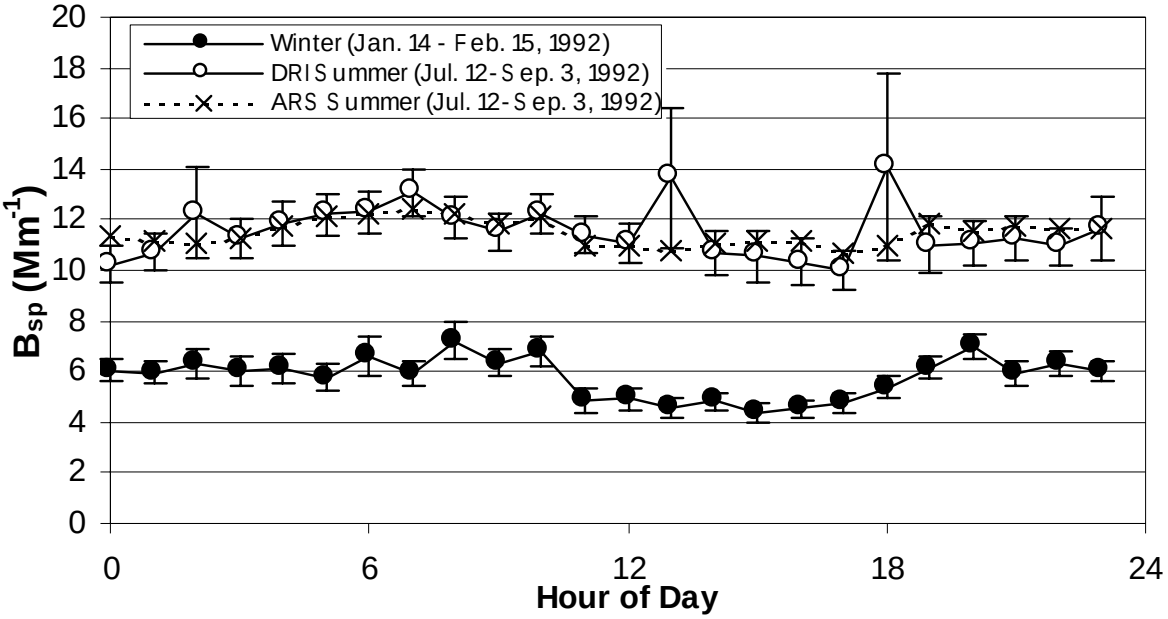

Figure 5-7 Diurnal variation of light scattering by particles measured at Meadview AZ.

5.4.2 Particle Light Scattering

During both the winter and summer intensive studies, DRI operated a nephelometer at Meadview to measure the scattering of light by particles (b_{sp}). ARS also deployed a nephelometer at Meadview during the summer intensive study. Data from the both nephelometers were adjusted to represent only the light scattering due to particles by subtracting the Rayleigh component from the nephelometer signal. (Note that a consistent data validation protocol was not established for the DRI nephelometer measurements so all of the data was labeled as suspect in the MOHAVE database.)

The nephelometer signals in Figure 5-8 behave similarly to the transmissometer signals in that the summertime measurements had greater temporal fluctuations than the wintertime measurements. Occasional high one hour nephelometer readings up to (150 Mm^{-1}) were observed during the summertime with the DRI nephelometer. It is unlikely that these peaks were representative of ambient particle scattering since they were not detected simultaneously with the ARS nephelometer or the transmissometer (Figure 5-5).

Average diurnal patterns were calculated for the nephelometer data in Figure 5-7. High standard errors were observed at 0200, 1300, and 1800 for the DRI summertime diurnal signal. These points coincide with the occurrence of individual high one hour readings and are not representative of the typical diurnal behavior of the particle scattering.

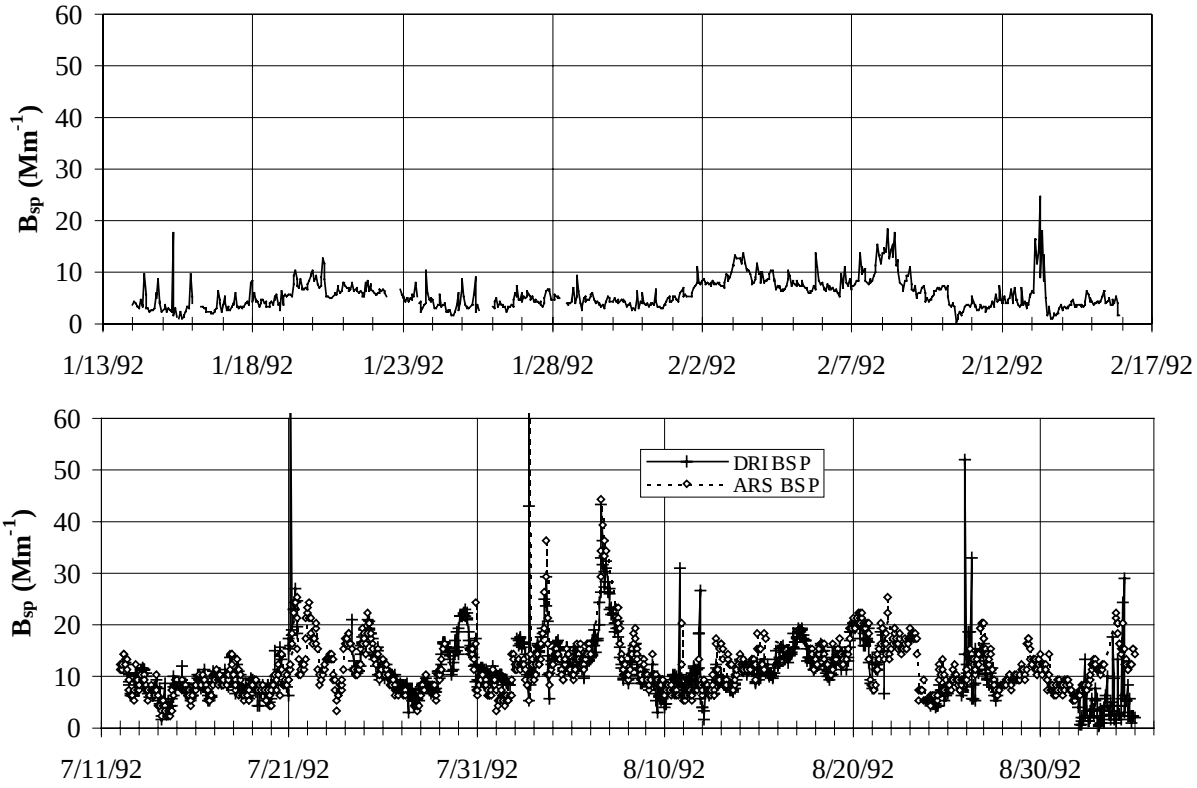

Figure 5-8 Time series of particle light scattering (b_{sp}) at MEAD.

As with the transmissometer measurements at GRCA and GRCW, diurnal patterns in the nephelometer signal peak in the morning between 0500 and 1000 during both the winter and summer intensive studies. The amplitude of the nephelometer diurnal pattern was ~ 2 Mm^{-1} which is less than that observed by the transmissometer.

5.4.3 Particle Light Absorption

Light absorption by particles was measured on aerosol filters collected at 12-hour intervals. While consensus has not been reached on exactly how the b_{ap} measurement relates to the true particle light absorption (see Section 4), the measured b_{ap} signal should have the same relative behavior of the true particle light absorption. Measurements of b_{ap} were conducted at Meadview, Hopi Point on the rim of the Grand Canyon, and Indian Gardens within the canyon. The particle absorption data is shown in Figure 5-9. Particle light absorption was higher in the canyon (INGA) than on the rim (HOPO) for an extended episode between 1/24/92 to 1/30/92. On average, b_{ap} was higher in the summer than in the winter by ~3 Mm^{-1}. Elevated levels of b_{ap} in excess of 15 Mm^{-1} were observed at HOPO for 4 periods during the summer intensive study. Differences between day and night samples of b_{ap} were not significant in either winter or summer at all sites.

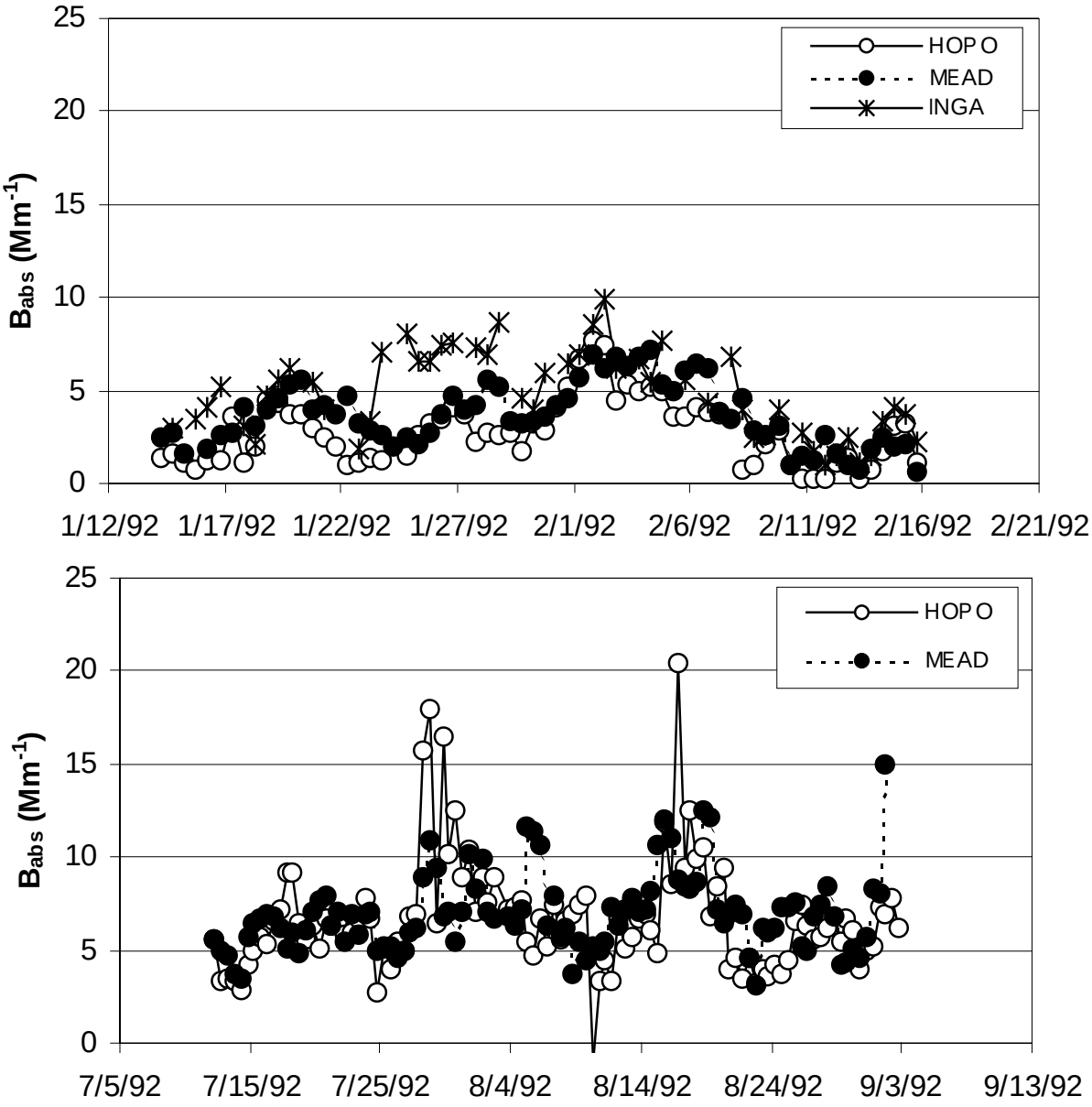

Figure 5-9 Time series of measured b_{abs} from 12-hour duration filters.

5.4.4 Calculating Total Extinction from Components

Sections 5.4.1 – 5.4.3 reviewed measurements of total extinction (b_{ext}), particle scattering (b_{sp}), and particle absorption (b_{abs}). Hasan and Lewis (1983) have carried out theoretical calculations to show that because of the forward angle truncation error of the nephelometer, it underestimates the coarse mass scattering (CMS) by about a factor of 2. White et al., (1994a) were able to show from transmissometer derived total scattering and nephelometer measurements of fine and coarse

particle scattering that the nephelometer underestimates scattering by particles greater than 2.5 μm by about a factor of 2.

Coarse mass (CM), b_{ext}, b_{sp}, and b_{abs} data are available from Meadview during the summer intensive. Since the extinction of light by gases is also known, a balance can be performed between total extinction and its measured components. The coarse mass scattering efficiency of 0.6 m^2/g is taken from a literature review by Trijonis and Pitchford (1987). The coarse mass scattering (CMS in Mm^{-1}) is then calculated as:

$$CMS = 0.6[CM] \qquad (5\text{-}2)$$

where [*CM*] is coarse mass in $\mu g/m^3$. Figure 5-10 shows a time series of the sum of b_{sg} (10.6 Mm^{-1} based on air density at Meadview), b_{abs} (IMPROVE sampler), b_{sp} (ARS nepelometer), and CMS/2 (IMPROVE sampler) along with the measured total extinction b_{ext} at Meadview. Note that data for some sampling periods are not shown in the figure.

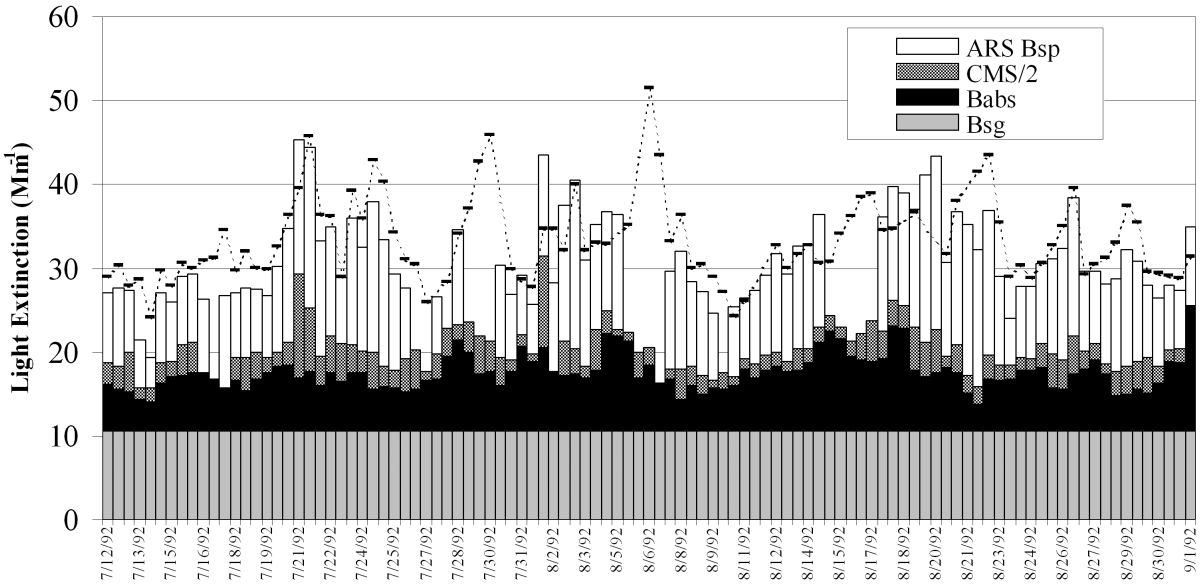

Figure 5-10 Extinction balance comparison of the sum of b_{abs}, b_{sg}, $b_{sp,}$ and CMS/2 with total b_{ext} at MEAD during the summer intensive study.

For sampling periods where all 4 observations are valid, the calculated extinction (b_{sg} + b_{abs} + b_{sp} + CMS/2) was regressed against the observed extinction (Figure 5-11). Light extinction was also calculated using an alternate approximation for b_{ap}. This approximation assumes that elemental carbon is the only light absorbing species, with a mass absorption efficiency of 10 m^2/g (i.e. b_{ap} = 10 [EC]). These calculated extinction values (black circles in Figure 5-11) are lower that the observed values by approximately 5 Mm^{-1}. Malm et al. (1996) and Huffman (1996b) presented evidence that this discrepancy is due to absorption by species associated with high temperature organic carbon (by TOR analysis) as well as soil aerosol.

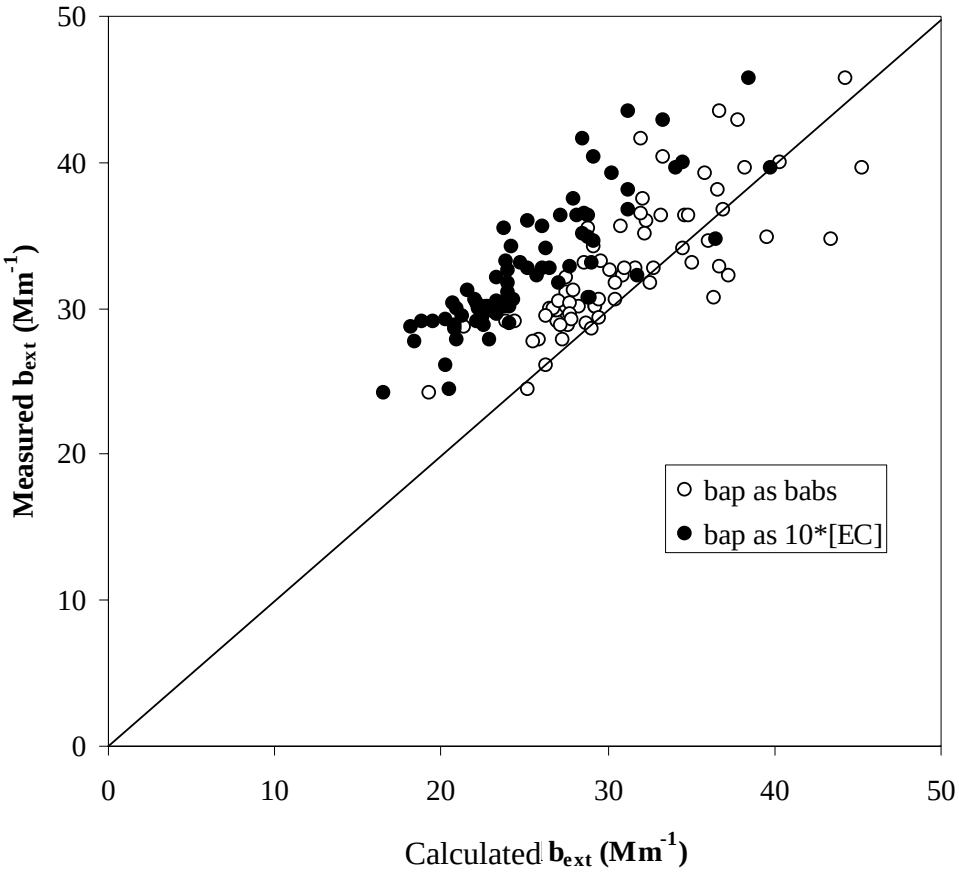

Figure 5-11 Comparison of measured extinction with calculated extinction (b_{sg} + b_{sp} + CMS/2 + b_{ap}). The open circles were calculated using $b_{ap} = b_{abs}$. The closed circles were calculated using b_{ap} = 10 [EC]. The line is the 1:1 line.

An alternative explanation for the disagreement between the measured extinction and the extinction calculated with the b_{ap} = 10 [EC] formulation is that excess extinction was measured by the transmissometer. This could have resulted from an incorrect value for the effective lamp strength caused by problems with transmissometer alignment or calibration (White, 1993).

This perspective is reinforced by Figure 5-12, which compares two measurements of extinction – b_{ext} by the transmissometer and b_{ap} and b_{sp} by nephelometer and integrating plate, respectively. The two sets of measurements, which are well correlated (r^2 = 0.79 for 77 points), should agree except for the tendency of the nephelometer to underestimate the effect of coarse particle scattering. In fact, they differ by a relatively constant offset of about 5 $^{Mm-1}$ over the entire range. The offset does not correlate with the coarse mass concentration (r^2 = 0.001). This suggests that one of the measurement techniques has a constant error.

Resolution of these discrepancies cannot be definitively achieved using the b_{abs} measurements as the appropriate representation of b_{ap} since these measurements may be too high by a factor of 2 (see Section 4.1.3). Consequently, MPP contributions to total extinction will be estimated using both the transmissometer measured extinction and the chemically calculated extinction using b_{ap} = 10 [EC] (to be discussed in Section 6.2)..

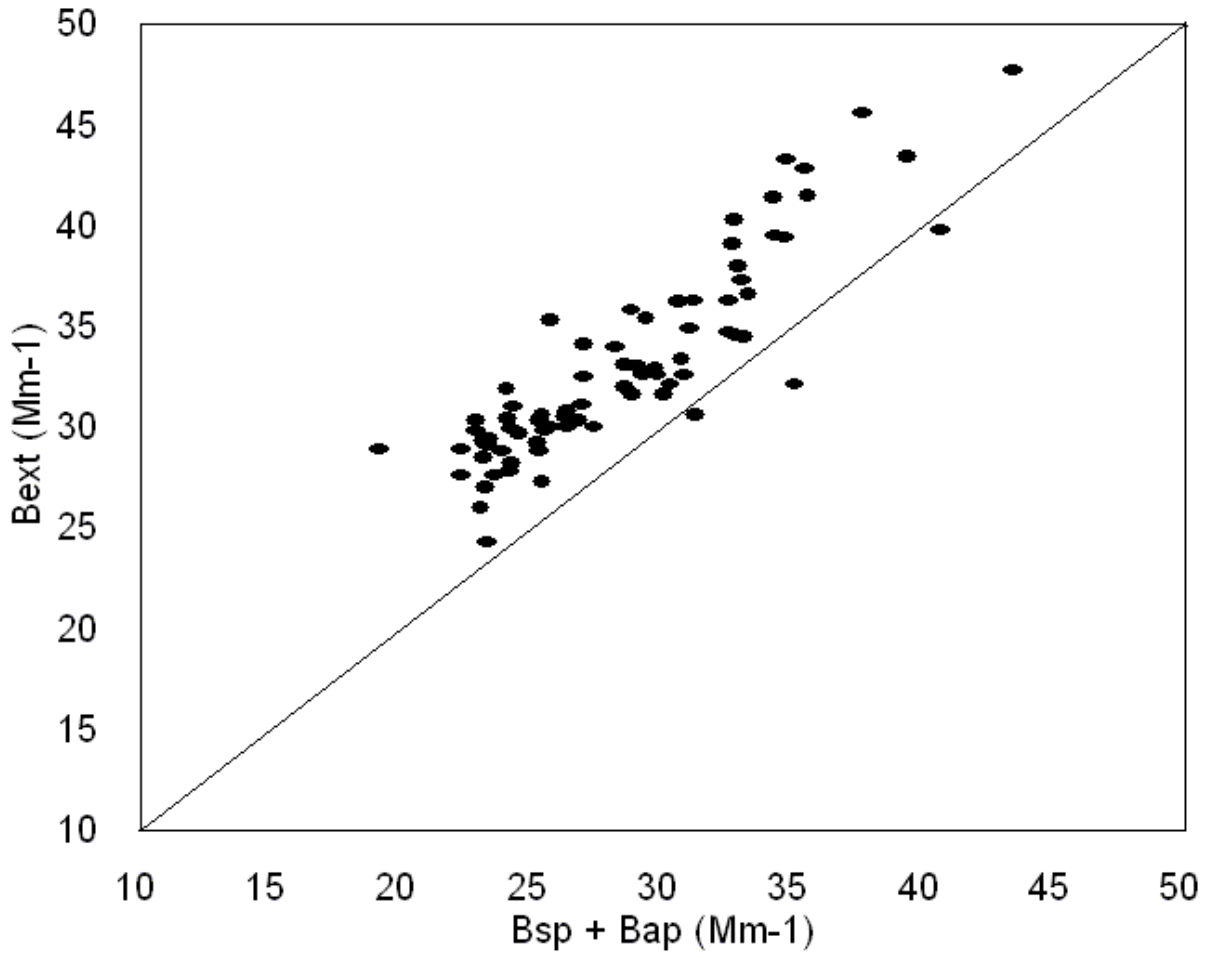

Figure 5-12 Comparison of two measurements of light extinction. The line is the 1:1 line.

5.5 Spatial Variability of Light Extinction and Its Components.

The components of light extinction vary in relative importance over the study region. Figure 5-13 show the summertime spatial distribution of the components of light extinction as measured by nephelometer and integrating plate method on fine aerosol filters. The values plotted in the figure are the median values of b_{sp}, b_{sg} (Rayleigh), and b_{sp} from each location during the summer intensive study. The sizes of the pie charts qualitatively indicate the magnitudes of the median calculated extinction observed at these sites.

The figure shows that near Los Angeles at Tehachapi Pass (TEHA) and Cajon Pass (CAJO), particle scattering (b_{sp}) accounts for more than half the light extinction. The fractional contributions of particle scattering and particle absorption are lower at Meadview (MEAD) than at the remaining sites due to the greater relative effects of Rayleigh scattering at Meadview. Particle absorption (b_{ap}) accounts for between 1/3 to 1/4 of the total extinction across the network. Total extinction decreases from southwest to northeast.

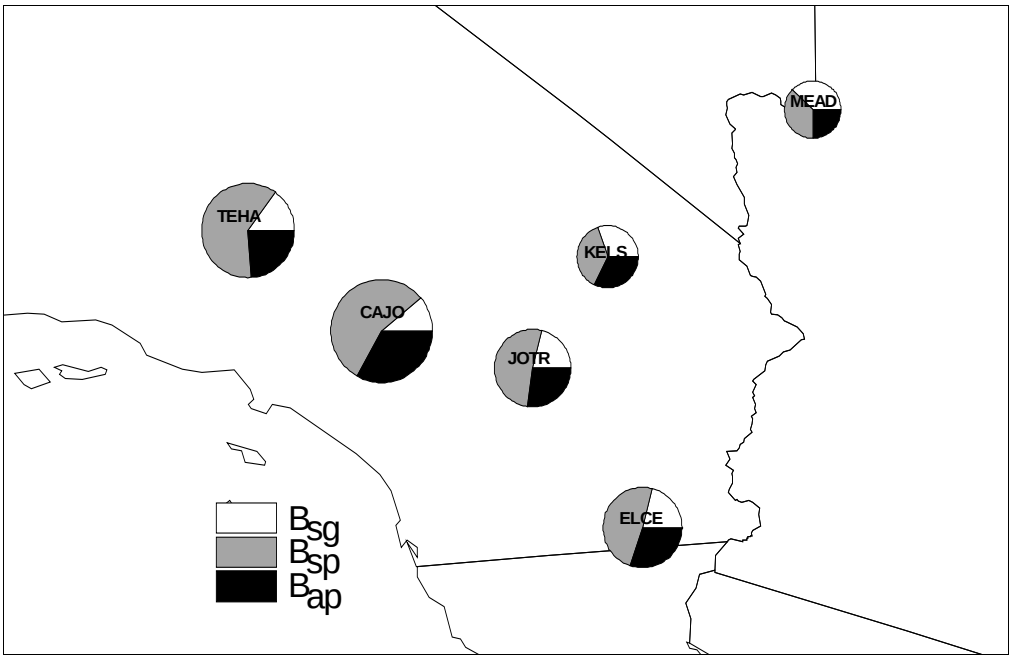

Figure 5-13 Map of summertime calculated light extinction.